REPORT DOCUMENTATION PAGE

Form Approved OMB NO. 0704-0188

1. REPORT DATE (DD-MM-YYYY)	2. REPORT TYPE	3. DATES COVERED (From - To)
01-03-2022	Final Report	4-Dec-2020 - 3-Dec-2021

4. TITLE AND SUBTITLE
Final Report: Dynamic Mechanical Analysis of Shear-Jammed Suspensions

5a. CONTRACT NUMBER
W911NF-21-1-0038

5b. GRANT NUMBER

5c. PROGRAM ELEMENT NUMBER
611103

6. AUTHORS

5d. PROJECT NUMBER

5e. TASK NUMBER

5f. WORK UNIT NUMBER

7. PERFORMING ORGANIZATION NAMES AND ADDRESSES
University of Chicago
5801 South Ellis Avenue

Chicago, IL 60637 -5418

8. PERFORMING ORGANIZATION REPORT NUMBER

9. SPONSORING/MONITORING AGENCY NAME(S) AND ADDRESS (ES)
U.S. Army Research Office
P.O. Box 12211
Research Triangle Park, NC 27709-2211

10. SPONSOR/MONITOR'S ACRONYM(S)
ARO

11. SPONSOR/MONITOR'S REPORT NUMBER(S)
77388-MS-RIP.1

12. DISTRIBUTION AVAILIBILITY STATEMENT
Approved for public release; distribution is unlimited.

13. SUPPLEMENTARY NOTES
The views, opinions and/or findings contained in this report are those of the author(s) and should not contrued as an official Department of the Army position, policy or decision, unless so designated by other documentation.

14. ABSTRACT

15. SUBJECT TERMS

16. SECURITY CLASSIFICATION OF:			17. LIMITATION OF ABSTRACT	15. NUMBER OF PAGES	19a. NAME OF RESPONSIBLE PERSON
a. REPORT	b. ABSTRACT	c. THIS PAGE			Heinrich Jaeger
UU	UU	UU	UU		19b. TELEPHONE NUMBER 773-702-8604

RPPR Final Report
as of 01-Mar-2022

Agency Code: 21XD

Proposal Number: 77388MSRIP **Agreement Number: W911NF-21-1-0038**
INVESTIGATOR(S):

Name: Heinrich Jaeger
Email: jaeger@uchicago.edu
Phone Number: 7737028604
Principal: Y

Organization: **University of Chicago**
Address: 5801 South Ellis Avenue, Chicago, IL 606375418
Country: USA
DUNS Number: 005421136 EIN: 362177139

Report Date: 03-Feb-2022 Date Received: 01-Mar-2022
Final Report for Period Beginning 04-Dec-2020 and Ending 03-Dec-2021
Title: Dynamic Mechanical Analysis of Shear-Jammed Suspensions
Begin Performance Period: 04-Dec-2020 **End Performance Period:** 03-Dec-2021
Report Term: 0-Other

Submitted By: Heinrich Jaeger Email: jaeger@uchicago.edu
Phone: (773) 702-8604

Distribution Statement: 1-Approved for public release; distribution is unlimited.

STEM Degrees: 0 **STEM Participants:**

Major Goals: This DURIP grant enabled the acquisition of a rheometer with dynamical mechanical analysis capabilities for the purpose of investigation concentrated (‘dense’) suspensions of small solid particles dispersed in a fluid. Such suspensions exhibit complex behavior that is of fundamental scientific interest and at the same time opens up new avenues for applications in the area of mechanically responsive materials. In particular, such suspensions can undergo an abrupt increase in their resistance to movement and can even transform from a freely flowing to a rigid, solid-like state when impacted or sheared. This fully reversible fluid-to-solid transformation exhibits highly desirable energy dissipation properties due to the preponderance of frictional particle interactions. The goal of the project was to advance experimental capabilities by combining, in the same equipment, rheological characterization of dense suspensions in their unjammed, fluid state with dynamical mechanical analysis of the material as it is driven through the shear jamming transition into its solid-like state. These unique capabilities aided in the design of stress-adaptive suspensions in which the frictional interactions between particles are made programmable via light-responsive chemistries. Research enabled by the new experimental capabilities aimed to uncover the fundamental physical mechanisms underlying the stress-activated fluid-to-solid transformation in dense suspension and explored dynamically tunable energy dissipation properties for next-generation protective gear.

Accomplishments: please see the uploaded pdf document.

Training Opportunities: please see the uploaded pdf file

Results Dissemination: The initial research performed with the newly acquired instrument led to several papers that have been submitted but are not published yet. See uploaded pdf file.

Honors and Awards: Nothing to Report

Protocol Activity Status:

Technology Transfer: Nothing to Report

PARTICIPANTS:

Participant Type: PD/PI
Participant: Heinrich Jaeger

Person Months Worked: 1.00 **Funding Support:**
Project Contribution:
National Academy Member: N

Participant Type: Graduate Student (research assistant)
Participant: Michael van der Naald
Person Months Worked: 1.00 **Funding Support:**
Project Contribution:
National Academy Member: N

Participant Type: Postdoctoral (scholar, fellow or other postdoctoral position)
Participant: Grayson Jackson
Person Months Worked: 1.00 **Funding Support:**
Project Contribution:
National Academy Member: N

Partners

,

I certify that the information in the report is complete and accurate:
Signature: Heinrich Jaeger
Signature Date: 3/1/22 12:10PM

Contract Number: W911NF-21-1-0038

Dynamic Mechanical Analysis of Shear-Jammed Suspensions

PI: Heinrich Jaeger, University of Chicago

Grants Officer's Representative (GOR): Dr. Daniel P. Cole

Final Progress Report

Period of Performance: December 04, 2020, to December 03, 2021

Table of Contents

Scientific Progress and Accomplishments

Statement of the Scientific Problem Studied with the Help of the DURIP Grant

Concentrated, or 'dense', suspensions of small particles immersed in a carrier fluid exhibit a rich set of unconventional, non-Newtonian mechanical behaviors when subjected to external stresses [1, 2]. Understanding these behaviors is of fundamental scientific interest and at the same time highly relevant to the handling and processing of complex fluids such as slurries, including as extrusion and slip casting as well as advanced additive manufacturing. A suspension with long-ranged attractive forces among the particles typically behaves as a yield stress fluid, i.e., it will be solid-like, jammed at rest and only flow upon exceeding minimum applied stress, beyond which it exhibits flow behavior such as shear thinning and potentially also shear thickening. A suspension with a preponderance of short-ranged frictional contacts will be liquid-like at rest but can quite generically transform from a flowing state to a solid-like 'shear-jammed' state if the particle fraction is sufficiently large and a sufficiently large shear stress is applied. Thus, tuning the relative strengths of the long- and short-ranged interactions allows one to engineer the response of the material to stress [3, 4]. The hallmark of these two stress-activated transitions, solid-to-liquid for a yield stress fluid and liquid-to-solid for a shear jammed system, is that they are *completely reversible* once the stress is removed. While yielding and shear-jamming in suspensions have been traditionally studied in isolation since the microscopic mechanisms for the two were thought to be unrelated, they can be conceptually linked by viewing the rheological behavior as a consequence of microscopic constraints on interparticle motion that are either destroyed or created by stress [5]. *A new perspective is thus emerging that views concentrated suspensions as stress-responsive materials wherein reversible solid-fluid, fluid-solid, or even re-entrant solid-like transformations are controlled by constraints at the level of particle-scale interactions.*

One important aspect of research in the PI's lab has been to develop a better understanding of the role of particle surface chemistry for the purpose of controlling these constraints and thus for designing the macroscale stress response of dense suspensions. We aim to obtain a much more detailed picture of the mechano-chemical scenario at molecular and nanometer scales, when particles are sheared into contact, and to identify its signatures in the macroscale observed flow properties.

Particle-laden fluids that can adapt smartly to applied stress have been championed for use in responsive protective wear and body armor that is flexible under normal conditions, yet can rigidify upon impact [6-10]. Similar principles underlie the design of puncture-resistant fabrics that protect against needlestick injuries [11] or against micrometeorites prevalent in low-earth orbit [12], as well as the development of special electrolytes for safety-enhanced batteries [13] or of rate-activated 'dynamic ligaments' to improve strapping of eyeware or helmets to the wearer's head [14, 15]. The fact that suspensions revert back to their fluid state after applied stresses are removed has also made them interesting as self-healing materials [16]. Taken together, these aspects make this research relevant to ARO needs. *In particular, the understanding gained in controlling particle-level interactions has the potential to open up new avenues for designing and even programming the response of suspensions to applied stress.*

Description of the Hardware Acquired and Installed

The equipment package acquired through the DURIP grant consisted of an Anton Paar MCR702 rheometer together with upgrades that provide important additional functionality. In particular, we added a second motor drive as well as dynamic mechanical analysis (DMA) capability. The MCR-

702 enables us to measure both stress-controlled and shear rate-controlled rheology, and with the addition of the lower drive it allows us to study the response of materials to deformations beyond simple shear. This introduces experimental modalities uniquely capable of probing, and also manipulating, the solid-like properties of the shear-jammed state. Below we describe in more detail the initial research we have been able to perform with the upgraded Anton Paar MCR702 rheometer.

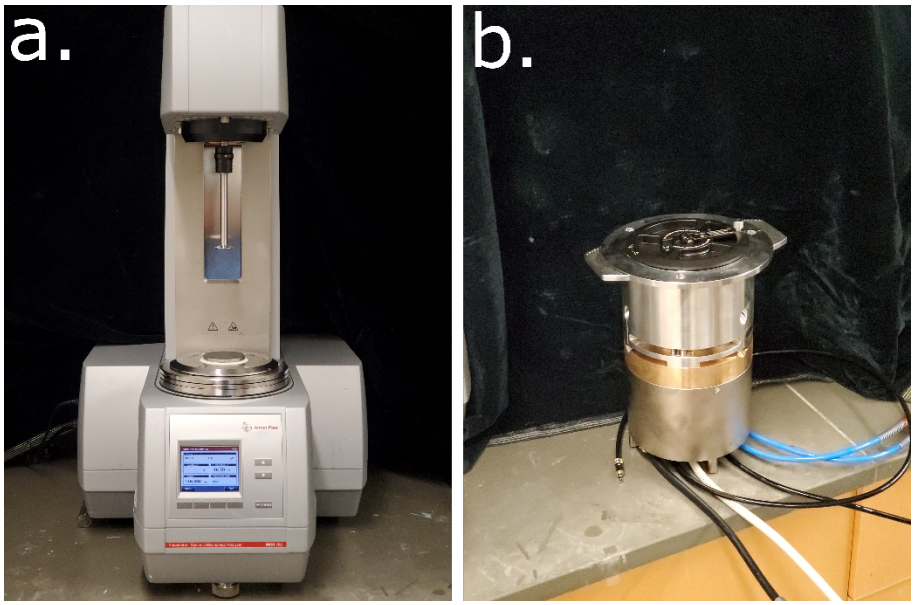

Figure 1. (a) The Anton-Paar MCR-702 rheometer. (b) The lower drive motor accessory.

Initial Research

Designing Stress-Adaptive Dense Suspensions using Dynamic Covalent Chemistry

This project has been a collaborative effort, led by the PI's postdoc Grayson Jackson, with the group of Stuart Rowan in the neighboring Pritzker School of Molecular Engineering (PME) and with Joseph Dennis from ARL (Combat Capabilities and Development Command), who works in with the Rowan group in the PME.

The non-Newtonian rheology of dense suspensions originates from microscopic constraints on interparticle motion [3, 5, 17-23]. Shear thinning arises from *stress-released* constraints which are broken upon increasing shear rate or stress, whereas *stress-activated* constraints (formed by increasing shear rate or stress) cause shear thickening. While the macroscopic viscosity in either case is constant at a given shear rate or stress, constraints are constantly breaking and reforming within a structurally dynamic network of non-covalent interparticle contacts. When the viscosity does evolve with time at a constant shear rate as in thixotropy (or antithixotropy), this signals the release (or formation) of constraints [24].While great strides have been made in understanding the constraint-based physics of dense suspensions, an emerging challenge is to connect microscopic constraints to specific chemical interactions [25].

To this end, prior work has focused on manipulating non-covalent chemical interactions such as van der Waals forces, solvation forces [26-28], depletion attraction [29, 30], steric stabilization [31-34], and hydrogen bonding [35-38]. These seminal studies provide a conceptual framework to

rationalize basic shear thickening or shear thinning behavior in terms of the relative strength of particle-particle and particle-solvent interactions (*i.e.* solubility) [27, 39]. If particle-particle attractions cannot be overcome by particle-solvent interactions, then the suspension possesses adhesive constraints at rest which are broken by shear (*shear thinning*). If the particle-solvent interaction strength is increased [27, 28, 39, 40] and the particle-particle attraction is diminished, e.g. by using surfactants [31, 32] or a covalently grafted steric barrier [33, 34], then particles are dispersed at rest, yet can form frictionally stabilized contacts under shear (*shear thickening*). The understanding from this prior work was established using simple non-covalent interactions, yet synthetic organic chemistry offers nearly limitless potential to tune particle-particle and particle-solvent interactions, thus presenting a new frontier for designing responsive dense suspensions.

Dynamic covalent chemistry (DCC) has recently emerged as a method to engineer stress-adaptive functional polymeric materials [41-47]. Like the non-covalent interactions described above, dynamic covalent bonds are able to dissociate and re-associate under equilibrium conditions, though typically they require a catalyst or external stimulus to access this reversibility [45]. When integrated into a dynamic covalent network (DCN) or covalent adaptable network (CAN), dynamic bonds enable structural reorganization under mechanical stress. This behavior is quite sensitive to the dynamic equilibrium constant (K_{eq}) [42, 48]. Past work also used interfacial DCC to integrate functionalized filler particles into crosslinked dynamic networks and studied the stress relaxation of these nanocomposites, though the DCCs used required exogenous catalysts [49-53]. As opposed to these nanocomposite systems with a crosslinked suspending matrix, dense suspensions possess a fluid matrix which allows particle migration and interparticle constraints to be formed or released under shear. While there have been studies of nanoparticle gels stabilized by dynamic covalent crosslinks [54-56], these works were primarily concerned with self-assembly rather than shear rheology. Within the context of a dense suspension, an ideal DCC would allow ambient temperature dynamic exchange without a catalyst as well as a readily tunable bond strength (K_{eq}), both of which are achievable using a specific class of thia-Michael (tM) reactions.

The tM reaction is the addition of a thiol to a thia-Michael accepting (tMA) electron-poor olefin to form a thioether adduct [57]. As demonstrated by foundational small molecule studies,[58-60] selection of certain substituents adjacent to the double bond lead to catalyst-free dynamic tM bonds at ambient temperatures. Examples of this include benzalcyanoacetate (BCA) and benzalcyanoacetamide (BCAm)-based tMAs. An advantage of BCA or BCAm-based tMAs is that K_{eq} can be tuned by varying the electron-donating/withdrawing nature of the R-substituents attached to the phenyl ring, which has been exploited in dynamic polymer networks [48], adhesives,[61] and hydrogels [62, 63].

Taking advantage of the catalyst-free, dynamic covalent bonds of the tM reaction with BCAm tMAs, presented here is the first study aimed at exploring the use of DCC in dense suspensions. Specifically, thiol-coated particles are dispersed in a fluid matrix comprised of a low molecular weight BCAm end-capped polymer. Importantly, this polymeric tMA solvent can form dynamic tM bonds at the particle surface to yield a dynamic brush layer (**Figure 2A**), with a bonding strength (K_{eq}) orders of magnitude larger than is achievable through a single hydrogen bond. While conventional non-covalent dense suspensions (with only hydrogen bonding interactions at the interface) (NCSs) exhibit shear thinning, these dynamic covalent suspensions (DCSs) exhibit antithixotropy wherein the viscosity reversibly increases under shear and relaxes upon shear cessation. Interestingly, the rheology of DCSs can be tuned between shear thinning and antithixotropy by varying K_{eq} of the tM bond, which in turn affects the dynamic graft density at

the particle surface. Moreover, it is shown that antithixotropy in DCSs arises from partial debonding of the particle grafts from the surface under shear and formation of polymer bridges between particles.

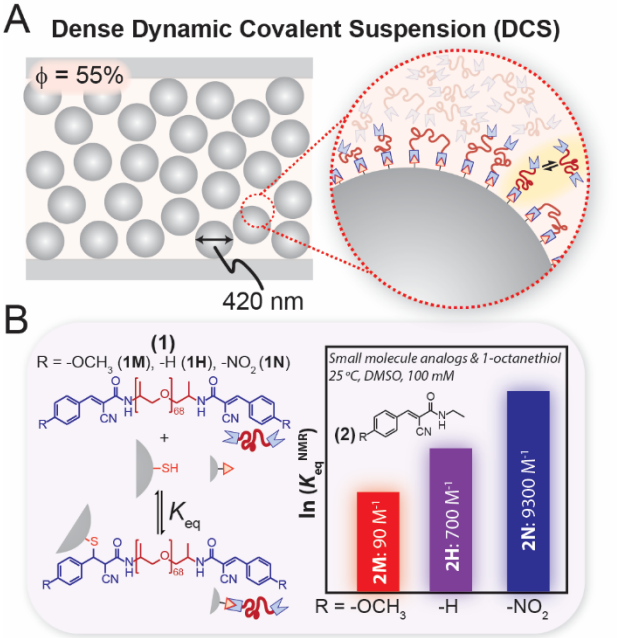

Figure 2. (*A*) Illustration depicting a dense dynamic covalent suspension (DCS). These high-volume-fraction (ϕ = 55%) DCSs contain particles which can form room temperature dynamic covalent bonds with the surrounding fluid polymer matrix, resulting in a bonded polymer graft layer which exchanges dynamically (*inset*). (*B*) Realization of DCSs using dynamic covalent thia-Michael (tM) chemistry. Chemical structure of ditopic poly(propylene glycol) benzalcyanoacetamide (BCAm) thia-Michael acceptors (tMAs) (**1**) with different R-substituents at the *para*-position of the b-phenyl ring, R = -OCH_3 (**1M**), -H (**1H**), -NO_2 (**1N**). These tMAs can form dynamic tM bonds at the surface of thiol-functionalized particles which exchange dynamically under ambient conditions without a catalyst. Small molecule analogs (**2M**, **2H**, or **2N**) were used to assess how temperature and chemistry affect the dynamic equilibrium constant (K_{eq}^{NMR}).

Material Synthesis and DCS Preparation. To realize the concept from Figure 1A in experiments, thiol-coated particles were prepared by grafting (3-mercaptopropyl)trimethoxysilane onto commercially available silica particles using literature procedures [64]. After surface functionalization, the particle diameter was 417 ± 30 nm and the particle surface was covered with 0.5 thiols/nm^2 as determined by NMR [64]. The tMA end-capped polymer was synthesized in 2 steps from an amine terminated M_n ~ 4000 g/mol poly(propylene glycol) (PPG) core. Acid-catalyzed condensation with cyanoacetic acid and subsequent Knoevenagel condensation with different benzaldehydes were used to synthesize 3 ditopic BCAm polymers. These are referred to by their R-substituents at the *para*-position of the b-phenyl ring: methoxy (R= -OCH_3) (**1M**), unsubstituted (R = -H) (**1H**), nitro (R = -NO_2) (**1N**) (**Figure 2B**).

To understand the baseline effect of temperature and R-substituent on the dynamic equilibrium constant (K_{eq}), small molecule analogs **2M**, **2H**, **2N** were synthesized and NMR was used to measure K_{eq}^{NMR} under 100 mM equimolar (with 1-octanethiol) conditions in DMSO-d_6 over the temperature range 25 – 77 °C. These experiments show that the value of K_{eq}^{NMR} can be tuned by over a factor of ~10^3 using temperature and chemistry: K_{eq}^{NMR} decreases upon heating and, at a constant temperature, shows a trend of **2N** > **2H** > **2M** (**Figure 2B**). As the reaction proceeds

through a charged enolate intermediate [60], reaction rates and overall equilibrium are expected to be impacted by solvent polarity. In addition to this, K_{eq} for DCSs represents polymeric tMA binding to surface thiols, and the entropic penalty for polymer chain stretching is not accounted for by K_{eq}^{NMR} and would lead to a lower effective K_{eq} in DCSs. With respect to these points, the small molecule controls are treated as estimates, however, the effects of temperature and chemistry from the model studies are expected to translate to DCSs.

DCSs at a particle volume percent (ϕ) of 55% were prepared with either **1M**, **1H**, or **1N** as the suspending solvent to yield DCS-1M, DCS-1H, or DCS-1N. A control non-covalent dense suspension (NCS-OH) was prepared at the same f and with the same particles but with 4000 g/mol hydroxyl-terminated PPG as the polymer matrix. From ϕ, particle density, and thiol surface coverage, it is estimated that [-SH] ~ 0.016 M and [tMA] ~ 0.46 M in the liquid phase of these suspensions, a nearly 30-fold excess of the tMA. In other words, the surface thiol group is the limiting reagent and leads to a high bonding fraction and subsequent polymer grafting at the particle surface. The tM adducts are envisioned to serve as a dynamic brush layer that depends on the dynamic bond strength (K_{eq}) with the remaining unbound tMAs serving as the carrier fluid (**Figure 2A**).

NCS and DCS Rheology. NCS-OH serves as a useful starting point to understand DCS rheology. NCS-OH exhibits conventional shear thinning where the viscosity decreases with increasing shear rate ($\dot{\gamma}$) (Figure 2A, black trace). In this figure, the reduced viscosity η_r is used to isolate the viscosity contribution of the particles from that of the suspending polymeric solvent. The forward (increasing) and backwards (decreasing) shear rate ramps overlay quite well for NCS-OH, illustrating no processing hysteresis and a viscosity which is independent of shearing time. As explored by others [21, 27, 39], shear thinning behavior in systems like NCS-OH can be understood as a solubility mismatch wherein hydrogen bonding or van der Waals forces between particle and solvent are not strong enough to overcome interparticle attractions. This leads to a stress-bearing (i.e. high viscosity) network of frictional, adhesive particle-particle contacts at rest which is disrupted by shear and leads to shear thinning [5, 32]. These stress-released interparticle contacts rapidly reform upon shear cessation and the suspension viscosity does not strongly depend on the shear history.

In stark contrast to the conventional shear thinning of NCS-OH, introduction of dynamic tM chemistry at the particle surface in DCS-1M leads to rich time-dependent rheology (**Figure 3A**). The measured viscosity on the forward shear rate ramp is low, while it is much higher upon the backwards shear rate ramp, indicating a strong hysteresis (Figure 2A, inset). However, the higher viscosity state decays upon shear cessation. Increasing the waiting time at each point in the shear rate ramp leads to a higher measured viscosity at low shear rates while the data were identical at higher shear rates (**Figure 3A**). At a constant shear rate, the viscosity evolves as a function of strain (γ) and shows an initial decay from the pre-sheared state followed by growth and a plateau at a high strain value (**Figure 3B**). The high strain value, which is interpreted as an approximate "steady state" viscosity plotted in Figure 2A, decreases with increasing shear rate or exhibits steady state shear thinning behavior. In line with the constant shear rate measurements, constant stress (*creep*) measurements of DCS-1M reveal a viscosity bifurcation [65, 66]: the viscosity diverges for $\sigma \leq 10$ Pa and flows for $\sigma \geq 100$ Pa. In other words, DCS-1M exhibits a yield stress, but only under shear. Qualitatively similar behavior was observed in constant shear rate and creep measurements of DCS-1H and DCS-1N. This reversible increase in viscosity indicates that these DCSs are antithixotropic, *i.e.*, the opposite of more conventional thixotropy, where shear forms a

stress-bearing particle network which returns to its equilibrium quiescent state upon shear cessation (**Figure 3C**) [24, 67].

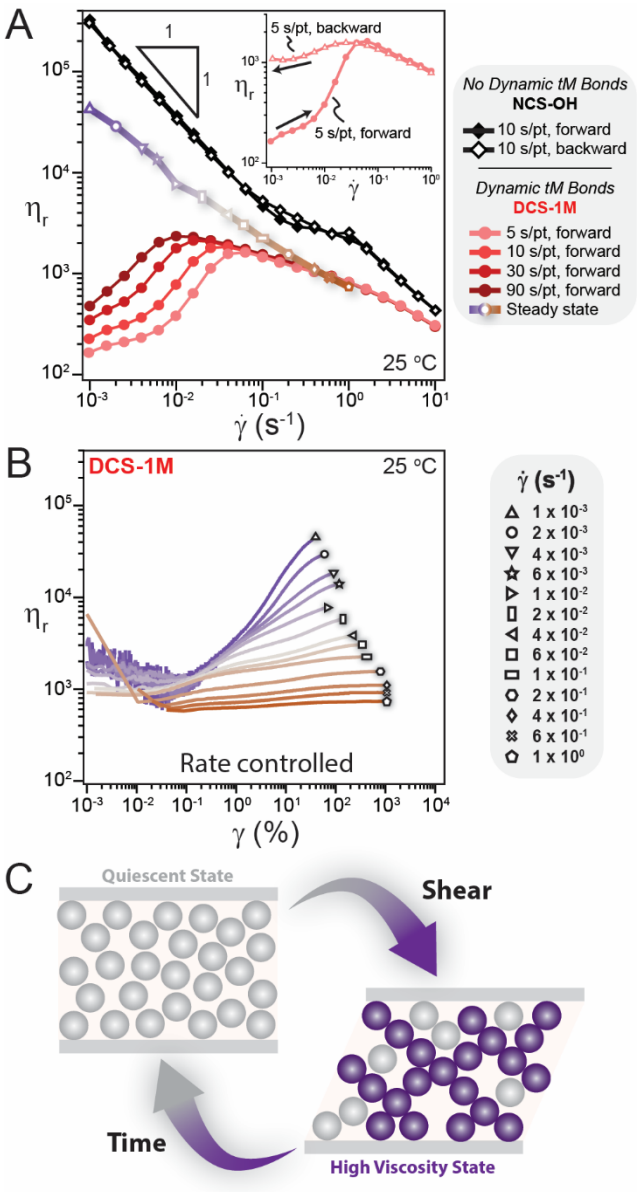

Figure 3. (*A*) Suspensions with only non-covalent hydrogen bonding interactions between particles and solvent (NCS-OH) exhibit reversible shear thinning. In contrast, dynamic covalent suspensions such as DCS-1M exhibit antithixotropy. Reduced viscosity η_r versus shear rate ($\dot{\gamma}$) for DCS-1M with different waiting times (*i.e.* number of seconds at each $\dot{\gamma}$ during a ramp in $\dot{\gamma}$) reveal that η_r increases as a function of shearing time and eventually approaches a steady-state. Similarly, comparison of the increasing (*forward*) and decreasing (*backward*) $\dot{\gamma}$ ramps reveal hysteresis (*inset*). (*B*) Evolution of η_r as a function of strain (γ) at a constant $\dot{\gamma}$ to reach a steady state. (*C*) Schematic depiction of antithixotropy, wherein shear reversibly transforms a low viscosity quiescent state into a higher viscosity state through the formation of a stress-bearing particle network (*purple*).

Small-amplitude oscillatory shear (SAOS) was used to track the decay of the complex viscosity (η^*) to understand how these shear-induced structures in DCSs relax upon shear cessation. These SAOS experiments were conducted immediately following the constant shear rate experiments shown in **Figures 3B.** DCSs subjected to lower shear rates, which typically had larger η_r plateau values prior to SAOS, exhibited a slower decay of η^*. In other words, more robust particle contact networks prior to shear cessation typically persisted longer once oscillatory shear was applied. It is worth pointing out that for shear-induced networks with similar η_r, the decay of η^* does not clearly correlate with the dynamic bond K_{eq} but does coincide with the trend in the viscosity of the dynamic tMA oil matrix (generally the slowest for DCS-1N, followed by DCS-1M, and then DCS-1H). This observation suggests that polymer diffusion also plays a role in the relaxation process.

Tuning Macroscopic Rheology with K_{eq}. As indicated by the small molecule studies (**Figure 2B**), K_{eq} and the dynamic brush layer density in DCSs can be systematically varied using temperature and chemistry. As such, temperature dependent rheology of DCSs was performed over the range 0 – 80 °C and shear rate ramps were used to identify antithixotropy or lack thereof (Figure 3A). As expected, NCS-OH exhibits reversible shear thinning or mild thixotropy over the entire temperature range (**Figure 4A**). However, the DCSs are much more sensitive to temperature and changes in K_{eq}. While DCS-1M exhibits antithixotropy at 10 °C and 30 °C, decreasing K_{eq} by heating ≥ 40 °C leads to strong and reversible shear thinning with a slope of nearly -1 on a log-log plot of η_r vs. $\dot{\gamma}$ (**Figure 4A**). At 70 °C it is apparent that η_r at a given shear rate is significantly larger even than that reached in the steady state at 25 °C. In other words, the stress-bearing particle network formed at rest at 70 °C is much stronger than that formed under shear at 25 °C. A similar transition from antithixotropy to shear thinning with mild thixotropy is observed when heating DCS-1H but the transition occurs when heating between 60 and 70 °C (**Figure 4A**). The area of the hysteresis loop generally decreases upon heating DCS-1M or DCS-1H, which could reflect a gradual transition between antithixotropy and shear thinning. The larger K_{eq} for DCS-1N leads to antithixotropy over the entire investigated range with an increasing mismatch between the forward and backward shear rate ramps. This trend for DCS-1N is particularly obvious at 70 °C where the viscosity at the end of the hysteresis loop is 3 orders of magnitude larger than its initial value.

Grouping the data shown in Figure 3A in terms of K_{eq}^{NMR} determined from small molecule analogs yields the rheological state diagram shown in **Figure 4B**. Despite the potential issues in translating K_{eq}^{NMR} directly to DCSs discussed above, the data in Figure 3B show a clear transition between antithixotropy and shear thinning at roughly the same value of K_{eq}^{NMR} (~50 M^{-1}) whether chemistry or temperature is used as the input variable. DCS-1N never reaches a low enough K_{eq}^{NMR} value to cross the threshold and thus only shows antithixotropy, whereas heating DCS-1M or DCS-1H leads to shear thinning. Antithixotropy in the DCSs is accompanied with viscoelastic or liquid-like behavior under SAOS whilst DCSs which show shear thinning are solid-like. It is worth pointing out that the estimated K_{eq}^{NMR} value for NCS-OH is orders of magnitude below the ~50 M^{-1} threshold and this system only exhibits reversible shear thinning.

The effect of K_{eq} in **DCSs a**nd transition from antithixotropy can be understood in terms of changes to the surface grafting density (**Figure 4C**), which alters particle stability in the surrounding homopolymer matrix in the quiescent, unsheared state. As detailed in the Supporting Information, K_{eq}^{NMR} can be converted into the fraction of bonded thiols (p). Again, this p-value likely overestimates the binding of polymeric tMAs to a surface due to the entropic penalty for polymer chain stretching but serves as a useful proxy for the dynamic graft density in DCSs (**Figure 4C**).

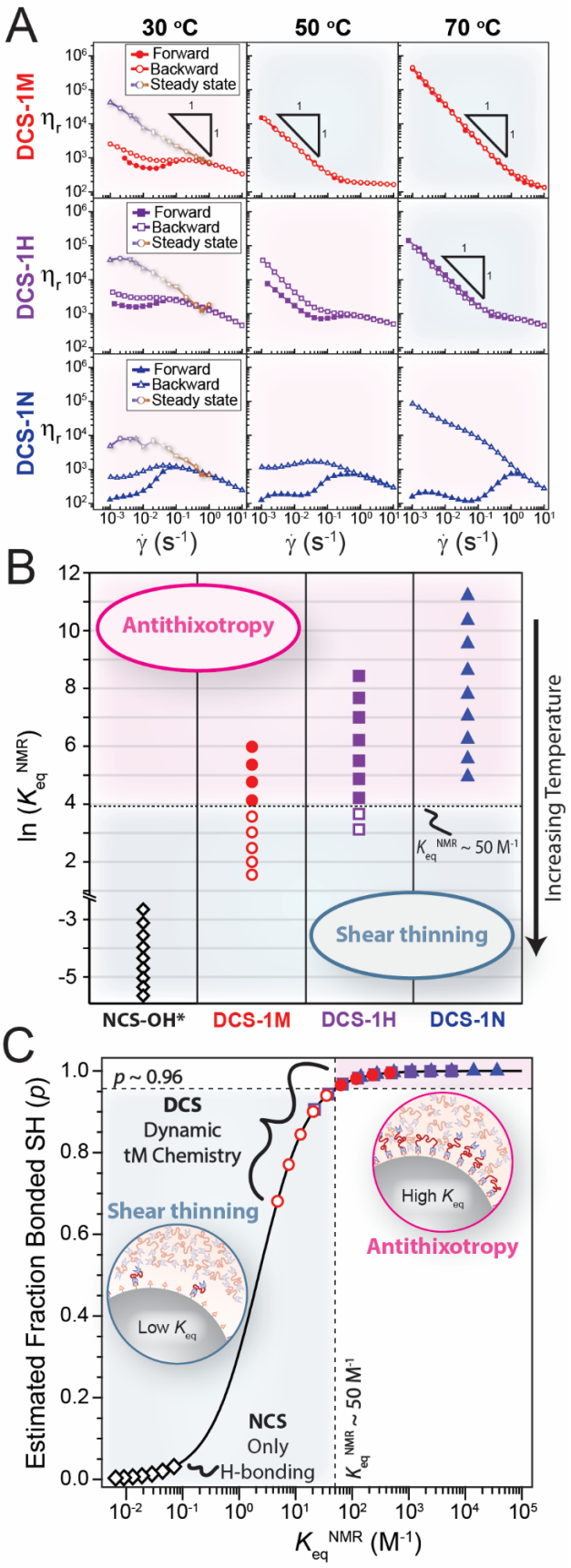

Figure 4. (*A*) Comparison of reduced viscosity (h_r) versus shear rate ($\dot{\gamma}$) for forward (*filled symbols*) and backward (*open symbols*) ramps reveal either hysteresis (antithixotropy) or no hysteresis (shear thinning). See Figure S13 for data at 10 °C. (*B*) Rheological state diagram for 0 – 80 °C for each system exhibiting a transition from antithixotropy (*filled symbols*) to shear thinning (*open symbols*) at $K_{eq}^{NMR} \sim 50\ M^{-1}$. The K_{eq}^{NMR} values for **NCS-OH** were estimated using literature data (see Table S2). (*C*) Relating K_{eq}^{NMR} to an estimated mole fraction of bound thiol (*p*) for **DCSs** and **NCS-OH** (solid line, see Supporting Information for details). Symbol identities are the same as in (*B*), with open symbols for shear thinning and filled symbols for antithixotropy. The *p*-value serves as a proxy for the brush layer density and shows a precipitous drop in the vicinity of the transition from antithixotropy to shear thinning.

Interestingly, p shows a precipitous drop in the vicinity of $K_{eq}^{NMR} \sim 50$ M^{-1} where **DCSs** transition from antithixotropy to shear thinning.

Such a change in nanoparticle dispersability with grafting density is precedented for covalently grafted polymer brushes. Polymer grafted nanoparticle (PGNP) stability in a polymer melt depends on grafting density and the relative length of the grafted and matrix polymer chains [68-70]. In the special case where the graft and matrix polymer chains are the same length (as is the case here), too low of a grafting density leads to partial wetting of the brush by the matrix and too high of a grafting density causes brush dewetting or a "dry" brush. Both cases lead to particle aggregation due to an entropic depletion attraction. In contrast, intermediate grafting density leads to a wet brush and provides a repulsive barrier and particle dispersal.

Extending these lessons from covalent brushes to dynamic covalent brushes, K_{eq} controls the time-averaged graft density (p) (**Figure 4C**). A large p leads to an initially dispersed quiescent state as evidenced by the relatively low initial h_r (Figure 3A) and liquid-like or viscoelastic SAOS response (Figure S15-16). Decreasing K_{eq} below ~ 50 M^{-1} leads to a precipitous drop in p which drives particle-particle contacts at rest,[27, 32, 39] as evidenced by the higher η_r, shear thinning under steady shear, and solid-like SAOS response (**Figure 4A**) [21, 69]. The system would be expected to be in the concentrated polymer brush (CPB) regime from a minimum graft density of ~0.07 chains/nm^2 to the maximum theoretical graft density of 0.5 chains/nm^2 set by the interfacial -SH density [71, 72].

The analogy to PGNPs applies to the initial quiescent state of the suspension (*i.e.* dispersed or aggregated), but does not answer why antithixotropy is observed for DCSs under steady shear. Antithixotropy requires shear-induced contacts, which could either be stabilized by polymer bridging or interparticle frictional contacts. Shear-induced polymer bridging would be possible in DCSs with ditopic tMAs and has been reported in "shake gels" of small ~20 nm particles with high molecular weight ~10^6 g/mol polymers [73-77]. On the other hand, antithixotropy is also possible without bridging interactions due to particle-particle frictional contacts, as seen in suspensions with high aspect ratio particles [66, 78, 79]. Frictional contacts would be possible in DCSs if the dynamic brush were to debond from the particle surface under shear and allow interparticle contacts.

To understand whether the primary mechanism for antithixotropy in DCSs involves polymer bridging or frictional particle-particle contacts, monotopic tMAs 3M and 3N (incapable of bridging) were synthesized (Figure 4A). As the molecular weight of the monotopic 3 is nominally half that of the ditopic 1, both systems possess roughly the same stoichiometric imbalance of tMA to thiol at a constant solids volume percent of $\phi = 55\%$. As shown in **Figure 5B**, DCS-3N exhibits shear thinning at low shear rates followed by shear thickening past ~1 s^{-1}. Essentially no hysteresis is observed for DCS-3N and the backwards flow curve almost exactly matches the steady state viscosity. In contrast, the same experimental conditions for DCS-1N lead to pronounced hysteresis over a larger shear rate range. The slight hysteresis at low shear rates observed for DCS-3N is also observed for a **NCS** prepared with $M_n \sim 2{,}000$ g/mol dihydroxy poly(propylene glycol), indicating that the dynamic covalent chemistry of monotopic tMAs does not induce hysteresis. Therefore, the pronounced hysteresis for ditopic tMAs is primarily the result of shear-induced polymer bridging.

Along the same lines, DCS-3N and DCS-3M equilibrate to their steady state viscosities at orders of magnitude lower strain values than DCS-1N or DCS-1M (**Figure 3**), respectively. Even after accounting for the changes in the tMA oil viscosity, the steady state η_r for the monotopic DCSs at

a given shear rate is approximately 20 times lower than for the ditopic DCSs (**Figure 5**). The larger steady state viscosities for ditopic DCSs indicates an additional attractive force between particles [21], which again points to shear-induced polymer bridging as the main mechanism for antithixotropy.

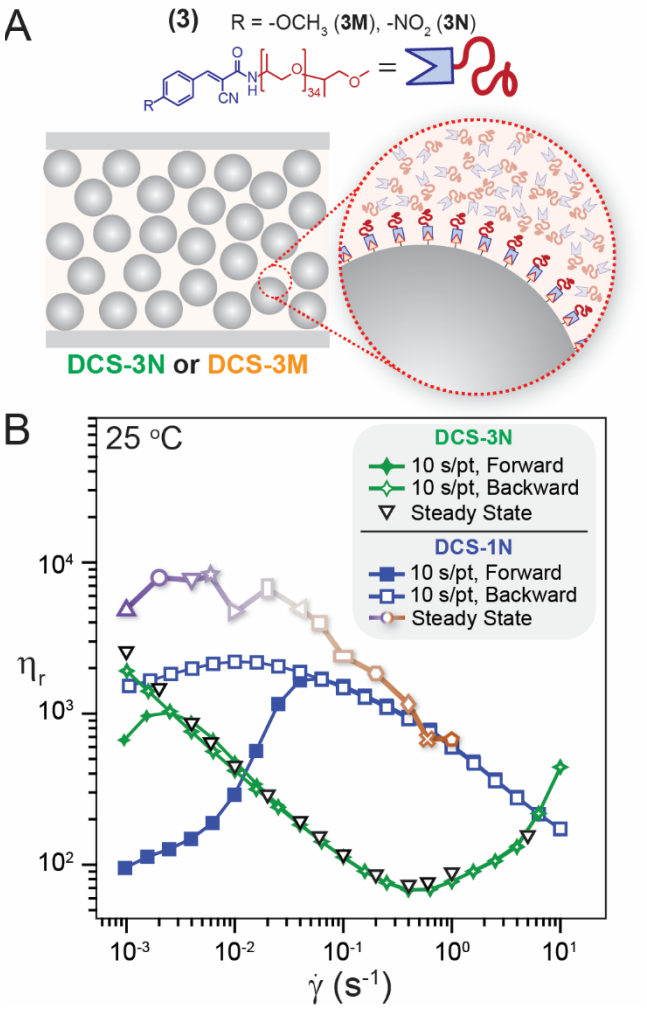

Figure 5. (A) A monotopic tMA 3N leads to DCSs without the possibility of shear-induced bridging between particles. (B) Reduced viscosity (η_r) for a forward-backward shear rate ($\dot{\gamma}$) ramp reveals mostly reversible behavior for DCS-3N, with a backward shear rate ramp which matches the steady state viscosity. This behavior contrasts greatly with that of the DCS-1N, which shows pronounced hysteresis. The steady state reduced viscosity for DCS-3N is also much lower than that of DCS-1N at a given shear rate.

While further experiments are needed to fully understand the effects of dynamic graft MW and stoichiometric imbalance, the comparison between monotopic and ditopic tMAs demonstrates that antithixotropy in ditopic DCSs primarily results from shear-induced polymer bridging (**Figure 6**). Such a mechanism requires not only polymer grafts capable of dynamically bridging between particle surfaces, but also exposed ("bare") surface sites which are dynamically revealed by tM debonding. In this scenario, the increasing hysteresis for DCS-1N at elevated temperatures could be due to the slight reduction in the dynamic graft density (p) which allows a larger number of polymer bridges. Additionally, Craig and coworkers have demonstrated that tensile force

accelerates the dissociation rate in dynamic metal-ligand complexes [80, 81], meaning that hydrodynamic shear stress at the particle surface could play a role in accelerating tM debonding and exposing surface sites under shear. In other words, p may decrease as shear rate increases. Such tensile forces could also be responsible for the steady state shear thinning behavior of the antithixotropic networks as a large enough shear stress releases particles from their microscopic tethers before they can reform. Finally, the decay of the antithixotropic state upon shear cessation correlates with the viscosity of the particle network before decay, with a lesser dependence on the viscosity of the dynamic tMA oil matrix. These data suggest that once the polymer bridges have stabilized the shear-induced network, contact relaxation requires particles to separate and reinfiltration of free tMA polymers to regenerate the repulsive brush layer (**Figure 6**).

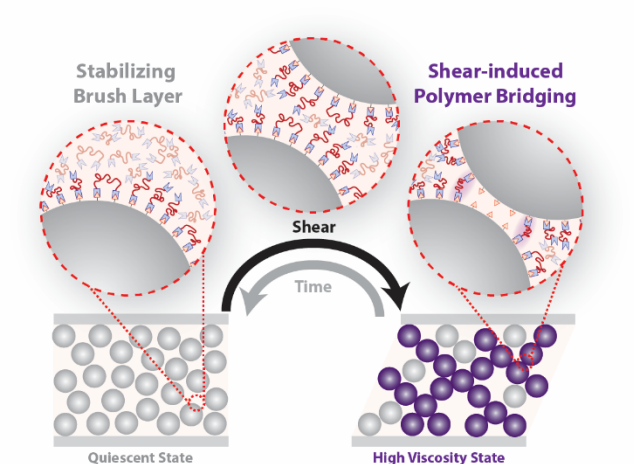

Figure 6. Cartoon illustration of the primary microscopic mechanism for antithixotropy in DCSs. Initially dispersed particles are forced into close contact by applied shear, during which the dynamic brush layer can partially debond and enable shear-induced polymer bridges which stabilize the high viscosity state. Removal of shear regenerates the sterically stabilized low viscosity quiescent state via re-bonding of free tMAs to reform a polymer brush.

Conclusions. Dynamic covalent thia-Michael chemistry at the particle-solvent interface has been shown to be a new approach to control the macroscopic flow behavior of dense suspensions. Small molecule control experiments were used to understand how temperature and chemistry control the equilibrium bonding constant (K_{eq}). DCSs at high K_{eq} exhibit antithixotropy, a rare non-Newtonian behavior where viscosity increases with shearing time and relaxes upon shear cessation. Decreasing K_{eq} led to more conventional rheology such as shear thinning. The changes in rheology with K_{eq} are interpreted in terms of the polymer graft density at the particle surface and subsequent wetting behavior by the surrounding homopolymer matrix. Finally, a monotopic tMA is used to elucidate the primary mechanism of DCS antithixotropy, namely that the dynamic covalent brush layer partially debonds under shear to enable polymer bridges between particles.

Incorporation of dynamic covalent grafts at a particle surface provides a new path forward towards the general design of antithixotropic materials which can controllably adjust their dissipation over time in response to mechanical inputs. Furthermore, the tunability of this particular system enables temperature to control the polymer graft density *in situ* and further toggle between two types of non-Newtonian behaviors, antithixotropy and shear thinning. This fine level of control over energy absorption and dissipation opens the door to new materials for vibration dampening, shock absorption, and impact mitigation.

A paper based on these results has been submitted to ACS Central Science.

Stress-activated Constraints in Dense Suspension Rheology

Given the large set of factors that can contribute to the non-Newtonian, stress-dependent behavior of concentrated particle suspensions, establishing a predictive link between microscale properties and macroscale observable ow behaviors has remianed a longstanding problem. A recent approach by Guy et al. to address this issue has been to classify the macroscale rheology not by focusing on the details of specific particle-particle forces, but rather on the general types of constraints that affect relative particle movement [5]. The promise of this approach lies in that the physical or chemical origin of any particular particle-particle interaction may matter far less than its net effect on the ability of neighboring particles to move with respect to one another. What remained to be shown, however, is which specific types of constraints are necessary for quantitative modeling of dense suspension rheology.

Using a combination of experiments and simulations we were able to demonstrate that quantitative modeling and prediction based on constraints is indeed possible. We introduced a new diagnostic framework to classify rheological ow curves in terms of whether sliding and rolling constraints on particle motion are present. Our approach provides insight into why particular particle-scale properties introduce additional constraints while others do not and unlocks a new connection between bulk rheology and nanoscale particle surface properties (**Fig. 7A**). This project was led by postdoc Abhinendra Singh, who is co-mentored by the PI and Juan de Pablo from the PME.

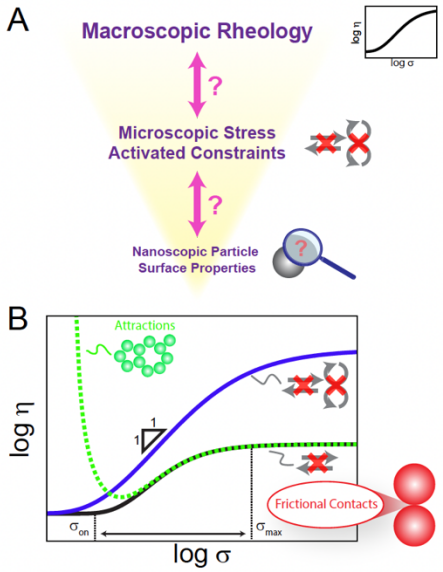

FIG. 7. (A) Shear thickening involves a hierarchy of length scales between macroscopic rheology, mesoscopic stress-activated constraints that hinder relative particle motion, and nanoscopic particle surface properties. (B) Sketch showing how different constraints affect shear thickening. Stress-activated sliding constraints alone lead only to continuous shear thickening (solid black line). Attractive central forces typically lead to a yield stress, without affecting shear thickening (dashed green line). Adding stress-activated rolling constraints can lead to discontinuous shear thickening (solid blue line).

During shear thickening the shear stress increases faster than the shear rate, leading to a net increase in viscosity η_r. For low solids volume fractions ϕ this increase is mild and occurs continuously as a function of applied shear, but for larger ϕ the viscosity can increase abruptly and dramatically when a critical rate is reached, behavior termed discontinuous shear thickening

(DST). For suffciently large ϕ and shear stress, these suspensions can furthermore transform into a shear-jammed (SJ), solid-like state, which melts back into a fluid once stress is released. Past work has established a strong foundation to understand the evolution of shear thickening toward DST and SJ, yet focused almost exclusively on stress-activated sliding friction, represented by a single coefficient for sliding friction μ_s [2, 3, 82-84].

In this picture, once the applied shear stress overwhelms the repulsive interparticle potential, unconstrained, hydrodynamically lubricated contacts transition to frictional contacts that prevent sliding. When viscosity η_r is plotted as a function of applied shear stress (**Fig. 7B**), this increase in the number of frictionally constrained particle-particle contacts manifests as shear thickening that starts at an onset stress and persists up to an upper limit, where the system has reached a state with all contacts frictional.

As the solids fraction ϕ gets closer to the onset packing fraction for jamming ϕ_J, the dependence of η_r on stress becomes steeper within the shear thickening regime, until DST is reached. In plots like **Fig. 7B**, DST is identified by a slope of unity, i.e., the viscosity is directly proportional to the stress. Increasing the sliding friction coefficient, reduces ϕ_J and thus, for given ϕ, brings the system closer to jamming. This in turn steepens the rise in viscosity with stress while at the same time increasing the final viscosity level that is reached in the large stress limit.

However, if only sliding constraints are considered, the effect on ϕ_J is rather small: it reduces the onset of jamming from a value which for monodisperse rigid spheres is equal to the random close-packing value RCP ~ 0.64 to no lower than ϕ_J ~0.56 even for $\mu_s = 1$ [85, 86]. This poses a serious problem for quantitative prediction, since experiments with rough spherical particles and also with specific chemical surface groups have demonstrated DST for packing fractions so low that the associated ϕ_J lies well below 0.56 and thus outside the range of current models based on just μ_s. Therefore, additional constraints beyond sliding are needed to properly capture the behavior of real suspensions.

Taking cues from modeling the rheology of dry granular materials [87], our recent simulations explored how additional stress-activated constraints on rolling affect shear thickening in dense suspensions [88] (**Fig. 8**). Interestingly, under the right conditions, already small additions of rolling friction were found to generate significant effects. At the same volume fraction where suspensions with only sliding constraints exhibit mild shear thickening, adding rolling friction can lead to DST, broaden the stress range over which shear thickening is observed, and increase the viscosity of the frictional state. In **Fig. 7B** this is shown by comparing the ow curves with (blue) and without (black) rolling friction. In the limit of infinite sliding and rolling friction the frictional jamming point drops as low 0.37. Short-ranged attractive particle-particle interactions that are not stress-activated and

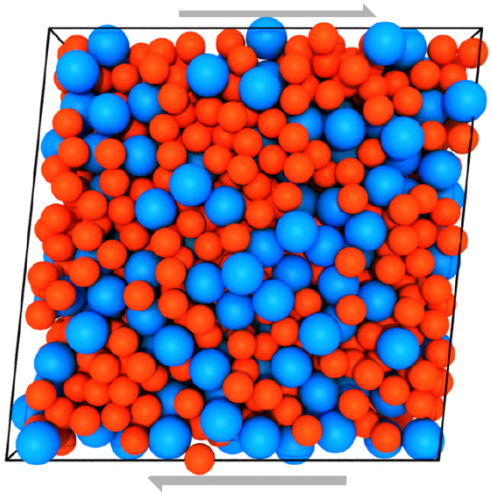

FIG. 8. Unit cell of the simulations, with 2000 total particles of two radii a (red) and 1.4a (blue). Each size particle makes up half of the particle volume fraction. This cell is replicated in all three directions and shearing is imposed by Lees-Edwards boundary conditions.

give rise to a yield stress can be included by simply adding them [3], as exemplified by the dashed green trace in **Fig. 7B** for the case without rolling friction.

Taken together, this opened up an opportunity we explored in this project: to model experimental suspension rheology quantitatively and understand how the combination of stress-activated sliding and rolling constraints, expressed in terms of an onset stress for frictional contact and coefficients for sliding and rolling friction, can be linked to particle-scale properties.

By comparing experimental data to state-of-the-art simulations we demonstrated how quantitative detail about the constraints that are operative over nanoscale distances at particle-particle contacts can be extracted from bulk measurements of the viscosity as a function of stress. We found that commonly studied suspensions, which vary widely in their composition, particle type and particle size, rather surprisingly exhibit nearly identical frictional constraints and that these constraints primarily are based on sliding friction between contacting particle surfaces (**Fig. 9**). We also explored deviations from such 'standard' suspension behavior, by focusing on large particle surface roughness and special particle surface chemistries, showing how this can lead to additional stress-activated constraints that hinder particle rolling.

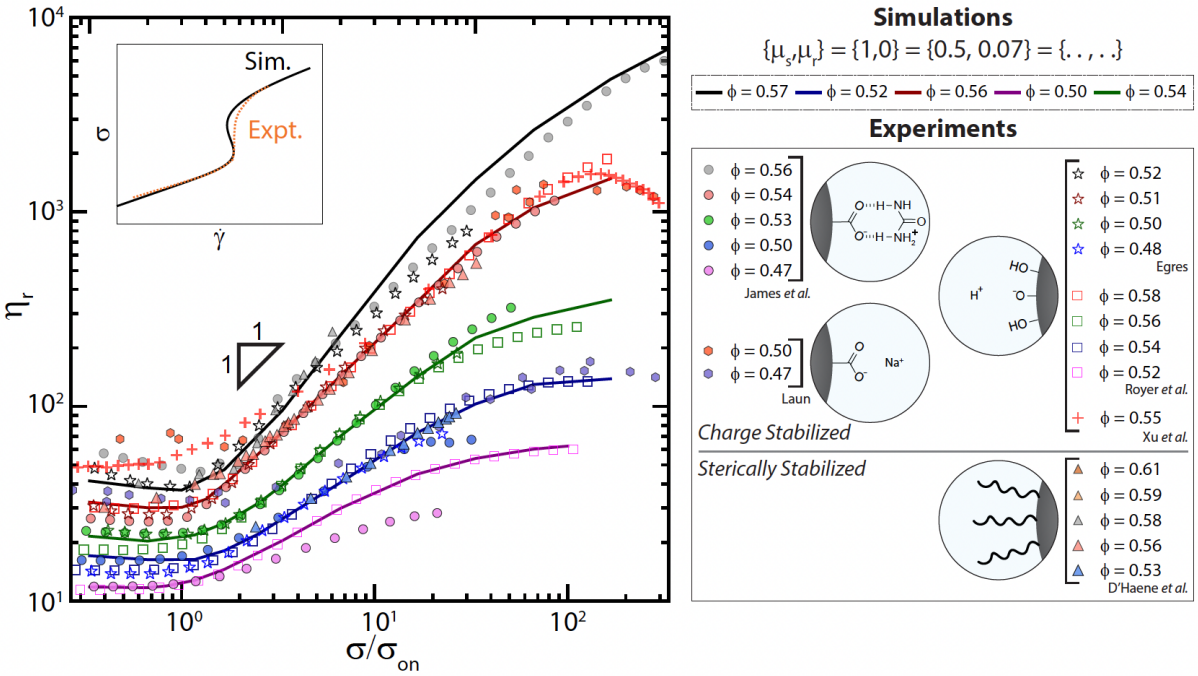

FIG. 9 Shear thickening of 'standard' particle suspensions shows nearly identical behavior as a function of packing fraction ϕ after scaling by the onset stress σ_{on}. Solid lines denote simulation data with sliding and rolling friction coefficients of 0.5 and 0.07, respectively. Symbols correspond to experimental data as indicated.

Our results highlight the power of a constraint-based approach for understanding and predicting the shear thickening behavior of diverse kinds of dense suspensions, including a wide range of different particle types and particle surface features. We found that two constraints on relative particle movement suffice for quantitative modeling, namely separate constraints on sliding and rolling that are activated when the local stress exceeds a threshold such that particles are coming into direct contact and experience friction forces. A central point in this approach is that each

constraint can represent a variety of different physical or chemical interactions giving rise to this friction. In particular, the approach allows one to translate ideas about chemical interactions typically developed under more dilute, closer to equilibrium conditions to these concentrated, out-of-equilibrium systems. In this project, constraints were implemented via associated friction coefficients for sliding and rolling, with magnitudes that provide an indicator of their relative strength. The combination of sliding and rolling constraints can affect the shear thickening behavior in highly nonlinear ways, where already small amounts of additional rolling friction can make an outsized contribution.

As a result, plots of the suspension viscosity as a function of applied shear stress can be viewed as a macroscopic reporter of stress-activated constraints that originate from contact interactions at the nanoscale. In particular, if the viscosity follows the 'standard' rheology in **Fig. 9**, then the sliding friction dominates and rolling friction can be neglected. If, however, the viscosity curve deviates from the 'standard' rheology, then the rolling and/or sliding constraints are stronger due to surface roughness or adhesive interactions such as hydrogen bonding between particle surfaces. Access to such detailed information about the relative contributions from sliding and rolling is exceedingly difficult to obtain from experiments that use scanning probe techniques, which necessarily focus on lateral sliding motion alone.

A paper based on these results is under review at Physical Review Fluids.

Using the Polymer Glass Transition to Thermally Tune Shear Jamming

This project was another collaboration with the group of Stuart Rowan in the PME. The effort was led by graduate student Chuqiao Elise Chen from the Rowan group and also involved graduate student Michael van der Naald and postdoc Grayson Jackson from the PI's group.

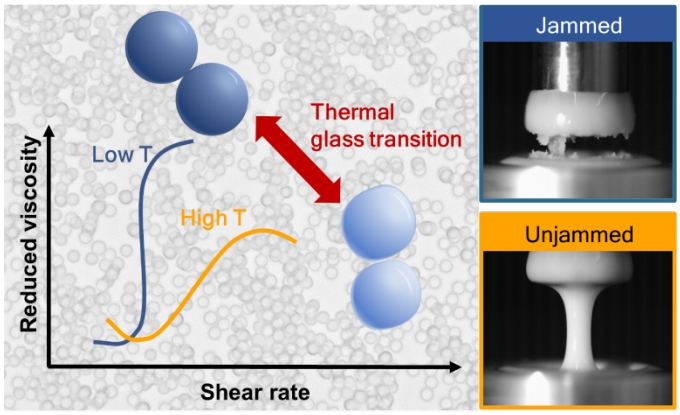

Figure 10: Left panel sketches the steady state rheology of our polymeric particle suspensions as the temperature is lowered to the glass transition temperature. The right panel shows the enhanced jamming capability of these suspensions as the temperature is lowered to the glass transition temperature.

Typical shear thickening suspensions use hard particles such as silica, PMMA, or some other easily stabilized particle type. With recent advances in particle synthesis techniques, it is now possible to make particles that have properties that can be tuned with external stimuli such as temperature or electric fields. We synthesized polymeric particles with a glass transition temperature close ambient temperature. We then used the MCR-702 to measure both the steady state rheology and

the shear jamming ability of suspensions of these particles as a function of temperature. We find that as the temperature approaches the glass transition temperature of the particles, the shear jamming and shear thickening are substantially enhanced, as sketched in **Figure 10** on the left. Shown on the right are two instances of using the capabilities of the rheometer to apply normal forces at a controlled, axial strain rate. By observing, with high-speed video, the details of how the suspension breaks up during tensile loading at a prescribed stress provides a direct indication of whether the suspension was in an unjammed, fluid state or in a shear-jammed, solid-like state. In this way, the DURIP grant enabled us to make some of the first explorations into suspensions comprised of particles that allow for *in-situ* tunable shear thickening by changing temperature.

A paper based on these results has been submitted and is under review.

Interfacial instabilities

Shear-induced interfacial fluid instabilities have been extensively studied in polymeric fluids, where they have been found to be the source of inaccuracies in experiments. Similar studies in dense suspensions are, however, lacking. Using the MCR-702 we have performed the first measurements of interfacial instabilities generated in dense suspensions under oscillatory shear. This project was led by Hojin Kim, a postdoc working jointly with both the PI's group and the group of Stuart Rowan in the PME.

We found that the pattern formed at the interface has a well-defined wavelength that depends on the applied oscillatory shear condition, as shown in **Figure 11**. Future work will focus on parameters that determine the onset of this instability and the wavelength of pattern formation, and on determining if this kind of instability can be mitigated or enhanced when applying an additional axial deformation. These instabilities are an important indicator for when the results from a parallel plate rheometer can be trusted, and therefore understanding their onset allows us to place fundamental bounds on the applicability of parallel plate rheology in dense suspensions.

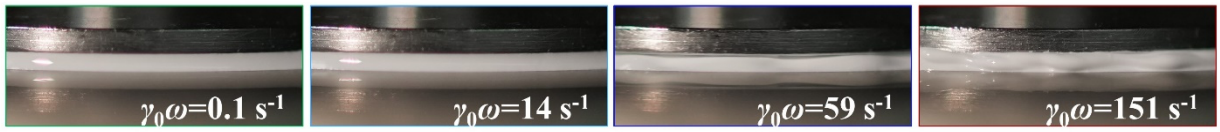

Figure 11. The evolution of the interfacial instability as shear is increased (left to right). Here γ_0 is the oscillatory shear amplitude and ω the oscillation frequency. In the first image on the left the applied shear rate is $\gamma_0\omega = 0.1s^{-1}$ and the suspension (in white) exhibits a smooth, flat interface. In the next image the shear rate is $\gamma_0\omega = 14s^{-1}$ and first deviations from a smooth interface are visible. The last two images show a fully developed instability that intensifies with increasing shear rate.

Orthogonal superposition rheology

A special capability of the MCR-702 with its second drive motor installed is that shear protocols can be programmed that simultaneously apply shear and axial deformation, i.e., apply modes of forcing along two orthogonal directions simultaneously. This makes it possible to investigate the stability of shear-induced flow structures and particle configurations inside a suspension. In particular, shearing a dense suspension will generate chains of contacting particles that are preferentially oriented along the compressive direction. These force chains are the origin of the very large stresses a suspension can support in the DST and SJ regimes. Application of stresses in the orthogonal direction has been shown to very significantly weaken such force chains and thus mitigate shear thickening [89]. This was demonstrated using a Couette geometry, where the

suspension was confined between two coaxial, cylindrical walls and the outer wall was rotated to supply shear stress while the inner wall was moved up and down vertically to generate stress orthogonal to the shear. Graduate student Michael van der Naald started a collaboration with the rheometer manufacturer (Anton Paar) to develop a similar protocol for the parallel plate geometry. In this geometry, parallel plates are rotated against each other to supply shear stress (as in **Fig. 11**) while their separation if modulated to generate the orthogonal, axial forcing. Initial measurements showed that shear with the addition of a gentle axial stress leads to lower viscosity, as expected from the earlier work with the Couette geometry [89]. However, with stronger applied axial stress we found that one can attain states that exhibit strongly enhanced viscosity. This demonstrates that the viscosity of a dense suspension subjected to orthogonal forcing is a more complex function of the magnitude and the direction of applied stresses than thought previously. Further work investigating orthogonal stress superposition is currently underway.

Personnel Participating in Equipment Setup and Initial Research

The rheometer was installed by graduate student Michael van der Naald and postdoc Grayson Jackson from the PI's research group. The following graduate students and postdoctoral scholars performed research on the instrument (PME = Pritzker School of Molecular Engineering at the University of Chicago):

Chuqiao Elise Chen (grad student with group of Stuart Rowan, PME)

Joseph M. Dennis (Combat Capabilities and Development Command, ARL)

Grayson Jackson (postdoc with PI's group)

Hojin Kim (postdoc jointly with PI's group and group of Stuart Rowan, PME)

Michael van der Naald (grad student with PI's group)

Abhinendra Sing (postdoc jointly with PI's group and group of Juan de Pablo, PME)

References Cited

[1] E. Brown and H. M. Jaeger, Shear thickening in concentrated suspensions: phenomenology, mechanisms, and relations to jamming, Reports On Progress In Physics 77, 046602 (2014). http://dx.doi.org/10.1088/0034-4885/77/4/046602

[2] M. M. Denn and J. F. Morris, Rheology of Non-Brownian Suspensions, Annual Review of Chemical and Biomolecular Engineering 5, 203-228 (2014). http://dx.doi.org/10.1146/annurev-chembioeng-060713-040221

[3] A. Singh, S. Pednekar, J. Chun, M. M. Denn, and J. F. Morris, From Yielding to Shear Jamming in a Cohesive Frictional Suspension, Physical Review Letters 122, 098004 (2019). http://dx.doi.org/10.1103/PhysRevLett.122.098004

[4] E. Brown, N. A. Forman, C. S. Orellana, H. J. Zhang, B. W. Maynor, D. E. Betts, J. M. DeSimone, and H. M. Jaeger, Generality of shear thickening in dense suspensions, Nature Materials 9, 220-224 (2010). http://dx.doi.org/10.1038/nmat2627

[5] B. M. Guy, J. A. Richards, D. J. M. Hodgson, E. Blanco, and W. C. K. Poon, Constraint-Based Approach to Granular Dispersion Rheology, Physical Review Letters 121, 128001 (2018). http://dx.doi.org/10.1103/PhysRevLett.121.128001

[6] Y. S. Lee, E. D. Wetzel, and N. J. Wagner, The ballistic impact characteristics of Kevlar (R) woven fabrics impregnated with a colloidal shear thickening fluid, Journal of Materials Science 38, 2825-2833 (2003). http://dx.doi.org/10.1023/A:1024424200221

[7] A. Srivastava, A. Majumdar, and B. S. Butola, Improving the Impact Resistance of Textile Structures by using Shear Thickening Fluids: A Review, Critical Reviews in Solid State and Materials Sciences 37, 115-129 (2012). http://dx.doi.org/10.1080/10408436.2011.613493

[8] A. Majumdar, B. S. Butola, and A. Srivastava, An analysis of deformation and energy absorption modes of shear thickening fluid treated Kevlar fabrics as soft body armour materials, Materials & Design 51, 148-153 (2013). http://dx.doi.org/10.1016/j.matdes.2013.04.016

[9] M. Hasanzadeh and V. Mottaghitalab, The Role of Shear-Thickening Fluids (STFs) in Ballistic and Stab-Resistance Improvement of Flexible Armor, Journal of Materials Engineering and Performance 23, 1182-1196 (2014). http://dx.doi.org/10.1007/s11665-014-0870-6

[10] S. Gurgen, M. C. Kushan, and W. Li, Shear thickening fluids in protective applications: A review, Progress in Polymer Science 75, 48-72 (2017). http://dx.doi.org/10.1016/j.progpolymsci.2017.07.003

[11] D. Firouzi, M. K. Russel, S. N. Rizvi, C. Y. Ching, and P. R. Selvaganapathy, Development of flexible particle-laden elastomeric textiles with improved penetration resistance to hypodermic needles, Materials & Design 156, 419-428 (2018). http://dx.doi.org/10.1016/j.matdes.2018.07.011

[12] C. D. Cwalina, C. M. McCutcheon, R. D. Dombrowski, and N. J. Wagner, Engineering enhanced cut and puncture resistance into the thermal micrometeoroid garment (TMG) using shear thickening fluid (STF) - Armor (TM) absorber layers, Composites Science and Technology 131, 61-66 (2016). http://dx.doi.org/10.1016/j.compscitech.2016.06.001

[13] Y. Ye, H. Xiao, K. Reaves, B. McCulloch, J. F. Mike, and J. L. Lutkenhaus, Effect of Nanorod Aspect Ratio on Shear Thickening Electrolytes for Safety-Enhanced Batteries, ACS Applied Nano Materials 1, 2774−2784 (2018). http://dx.doi.org/10.1021/acsanm.8b00457

[14] P. T. Nenno and E. D. Wetzel, Design and properties of a rate-dependent 'dynamic ligament' containing shear thickening fluid, Smart Materials and Structures 23, 125019 (2014). http://dx.doi.org/10.1088/0964-1726/23/12/125019

[15] E. L. Ballantyne, D. J. Little, and E. D. Wetzel, Rate-activated strapping for improved retention of protective eyewear during impact, Sports Engineering 20, 171-183 (2017). http://dx.doi.org/10.1007/s12283-017-0226-1

[16] R. P. Wool, Self-healing materials: a review, Soft Matter 4, 400-418 (2008). http://dx.doi.org/10.1039/b711716g

[17] C. S. Ness, Ryohei; Mari, Romain, The Physics of Dense Suspensions, arXiv preprint, arXiv:2105.04162 (2021).

[18] N. Y. C. Lin, B. M. Guy, M. Hermes, C. Ness, J. Sun, W. C. K. Poon, and I. Cohen, Hydrodynamic and Contact Contributions to Continuous Shear Thickening in Colloidal Suspensions, Physical Review Letters 115, 228304 (2015). http://dx.doi.org/10.1103/PhysRevLett.115.228304

[19] D. Bonn, M. M. Denn, L. Berthier, T. Divoux, and S. Manneville, Yield stress materials in soft condensed matter, Reviews of Modern Physics 89, 035005 (2017). http://dx.doi.org/10.1103/RevModPhys.89.035005

[20] M. M. Denn, J. F. Morris, and D. Bonn, Shear thickening in concentrated suspensions of smooth spheres in Newtonian suspending fluids, Soft Matter 14, 170-184 (2018). http://dx.doi.org/10.1039/c7sm00761b

[21] M. Nabizadeh and S. Jamali, Life and death of colloidal bonds control the rate-dependent rheology of gels, Nature Communications 12, 4274 (2021). http://dx.doi.org/10.1038/s41467-021-24416-x

[22] N. Fernandez, R. Mani, D. Rinaldi, D. Kadau, M. Mosquet, H. Lombois-Burger, J. Cayer-Barrioz, H. J. Herrmann, N. D. Spencer, and L. Isa, Microscopic Mechanism for Shear Thickening of Non-Brownian Suspensions, Physical Review Letters 111, 108301 (2013). http://dx.doi.org/10.1103/PhysRevLett.111.108301

[23] J. R. Royer, D. L. Blair, and S. D. Hudson, Rheological Signature of Frictional Interactions in Shear Thickening Suspensions, Physical Review Letters 116, 188301 (2016). http://dx.doi.org/10.1103/PhysRevLett.116.188301

[24] J. Mewis and N. J. Wagner, Thixotropy, Advances in Colloid and Interface Science 147-148, 214-227 (2009). http://dx.doi.org/https://doi.org/10.1016/j.cis.2008.09.005

[25] A. Singh, G. L. Jackson, M. van der Naald, J. J. de Pablo, and H. M. Jaeger, Stress-activated Constraints in Dense Suspension Rheology, arXiv preprint, arXiv: 2108.09860 (2021). http://dx.doi.org/

[26] M. van der Naald, L. Zhao, G. L. Jackson, and H. M. Jaeger, The role of solvent molecular weight in shear thickening and shear jamming, Soft Matter 17, 3144-3152 (2021). http://dx.doi.org/10.1039/D0SM01350A

[27] S. R. Raghavan, H. J. Walls, and S. A. Khan, Rheology of Silica Dispersions in Organic Liquids: New Evidence for Solvation Forces Dictated by Hydrogen Bonding, Langmuir 16, 7920-7930 (2000). http://dx.doi.org/10.1021/la991548q

[28] K. Ueno, S. Imaizumi, K. Hata, and M. Watanabe, Colloidal Interaction in Ionic Liquids: Effects of Ionic Structures and Surface Chemistry on Rheology of Silica Colloidal Dispersions, Langmuir 25, 825-831 (2009). http://dx.doi.org/10.1021/la803124m

[29] V. Gopalakrishnan and C. F. Zukoski, Effect of attractions on shear thickening in dense suspensions, Journal of Rheology 48, 1321-1344 (2004). http://dx.doi.org/10.1122/1.1784785

[30] N. Park, V. Rathee, D. L. Blair, and J. C. Conrad, Contact Networks Enhance Shear Thickening in Attractive Colloid-Polymer Mixtures, Physical Review Letters 122, 228003 (2019). http://dx.doi.org/10.1103/PhysRevLett.122.228003

[31] E. Brown, N. A. Forman, C. S. Orellana, H. Zhang, B. W. Maynor, D. E. Betts, J. M. DeSimone, and H. M. Jaeger, Generality of shear thickening in dense suspensions, Nature Materials 9, 220-224 (2010). http://dx.doi.org/10.1038/nmat2627

[32] J. A. Richards, R. E. O'Neill, and W. C. K. Poon, Turning a yield-stress calcite suspension into a shear-thickening one by tuning inter-particle friction, Rheologica Acta (2020). http://dx.doi.org/10.1007/s00397-020-01247-z

[33] B. M. Guy, M. Hermes, and W. C. K. Poon, Towards a Unified Description of the Rheology of Hard-Particle Suspensions, Physical Review Letters 115, 088304 (2015). http://dx.doi.org/10.1103/PhysRevLett.115.088304

[34] W. J. Frith, P. d'Haene, R. Buscall, and J. Mewis, Shear thickening in model suspensions of sterically stabilized particles, Journal of Rheology 40, 531-548 (1996). http://dx.doi.org/10.1122/1.550791

[35] N. M. James, E. Han, R. A. L. de la Cruz, J. Jureller, and H. M. Jaeger, Interparticle hydrogen bonding can elicit shear jamming in dense suspensions, Nature Materials 17, 965-970 (2018). http://dx.doi.org/10.1038/s41563-018-0175-5

[36] W. Yang, Y. Wu, X. Pei, F. Zhou, and Q. Xue, Contribution of Surface Chemistry to the Shear Thickening of Silica Nanoparticle Suspensions, Langmuir 33, 1037-1042 (2017). http://dx.doi.org/10.1021/acs.langmuir.6b04060

[37] J. Warren, S. Offenberger, H. Toghiani, C. U. Pittman, T. E. Lacy, and S. Kundu, Effect of Temperature on the Shear-Thickening Behavior of Fumed Silica Suspensions, ACS Applied Materials & Interfaces 7, 18650-18661 (2015). http://dx.doi.org/10.1021/acsami.5b05094

[38] H. M. Laun, Rheological properties of aqueous polymer dispersions, Die Angewandte Makromolekulare Chemie 123, 335-359 (1984). http://dx.doi.org/https://doi.org/10.1002/apmc.1984.051230115

[39] S. R. Raghavan, J. Hou, G. L. Baker, and S. A. Khan, Colloidal Interactions between Particles with Tethered Nonpolar Chains Dispersed in Polar Media: Direct Correlation between Dynamic Rheology and Interaction Parameters, Langmuir 16, 1066-1077 (2000). http://dx.doi.org/10.1021/la9815953

[40] P. N. Bourrianne, Vincent; Polly, Gatien; Divoux, Thibaut; McKinley, Gareth H., Unifying Disparate Experimental Views on Shear-thickening Suspensions, arXiv preprint, arXiv: 2108.09860 (2020).

[41] R. J. Wojtecki, M. A. Meador, and S. J. Rowan, Using the dynamic bond to access macroscopically responsive structurally dynamic polymers, Nature Materials 10, 14-27 (2011). http://dx.doi.org/10.1038/nmat2891

[42] C. J. Kloxin and C. N. Bowman, Covalent adaptable networks: smart, reconfigurable and responsive network systems, Chemical Society Reviews 42, 7161-7173 (2013). http://dx.doi.org/10.1039/C3CS60046G

[43] P. Chakma, L. H. Rodrigues Possarle, Z. A. Digby, B. Zhang, J. L. Sparks, and D. Konkolewicz, Dual stimuli responsive self-healing and malleable materials based on dynamic thiol-Michael chemistry, Polymer Chemistry 8, 6534-6543 (2017). http://dx.doi.org/10.1039/C7PY01356F

[44] B. B. Jing and C. M. Evans, Catalyst-Free Dynamic Networks for Recyclable, Self-Healing Solid Polymer Electrolytes, Journal of the American Chemical Society 141, 18932-18937 (2019). http://dx.doi.org/10.1021/jacs.9b09811

[45] S. J. Rowan, S. J. Cantrill, G. R. L. Cousins, J. K. M. Sanders, and J. F. Stoddart, Dynamic Covalent Chemistry, Angewandte Chemie International Edition 41, 898-952 (2002). http://dx.doi.org/https://doi.org/10.1002/1521-3773(20020315)41:6<898::AID-ANIE898>3.0.CO;2-E

[46] W. C. Yount, D. M. Loveless, and S. L. Craig, Small-Molecule Dynamics and Mechanisms Underlying the Macroscopic Mechanical Properties of Coordinatively Cross-Linked Polymer Networks, Journal of the American Chemical Society 127, 14488-14496 (2005). http://dx.doi.org/10.1021/ja054298a

[47] D. Xu and S. L. Craig, Strain Hardening and Strain Softening of Reversibly Cross-Linked Supramolecular Polymer Networks, Macromolecules 44, 7478-7488 (2011). http://dx.doi.org/10.1021/ma201386t

[48] K. M. Herbert, P. T. Getty, N. D. Dolinski, J. E. Hertzog, D. de Jong, J. H. Lettow, J. Romulus, J. W. Onorato, E. M. Foster, and S. J. Rowan, Dynamic reaction-induced phase separation in tunable, adaptive covalent networks, Chemical Science 11, 5028-5036 (2020). http://dx.doi.org/10.1039/D0SC00605J

[49] N. Sowan, L. M. Cox, P. K. Shah, H. B. Song, J. W. Stansbury, and C. N. Bowman, Dynamic Covalent Chemistry at Interfaces: Development of Tougher, Healable Composites through Stress Relaxation at the Resin–Silica Nanoparticles Interface, Advanced Materials Interfaces 5, 1800511 (2018). http://dx.doi.org/https://doi.org/10.1002/admi.201800511

[50] X. Chen, L. Li, T. Wei, D. C. Venerus, and J. M. Torkelson, Reprocessable Polyhydroxyurethane Network Composites: Effect of Filler Surface Functionality on Cross-link Density Recovery and Stress Relaxation, ACS Applied Materials & Interfaces 11, 2398-2407 (2019). http://dx.doi.org/10.1021/acsami.8b19100

[51] Y. Liu, Z. Tang, Y. Chen, C. Zhang, and B. Guo, Engineering of β-Hydroxyl Esters into Elastomer–Nanoparticle Interface toward Malleable, Robust, and Reprocessable Vitrimer Composites, ACS Applied Materials & Interfaces 10, 2992-3001 (2018). http://dx.doi.org/10.1021/acsami.7b17465

[52] A. Legrand and C. Soulié-Ziakovic, Silica–Epoxy Vitrimer Nanocomposites, Macromolecules 49, 5893-5902 (2016). http://dx.doi.org/10.1021/acs.macromol.6b00826

[53] E. Cudjoe, K. M. Herbert, and S. J. Rowan, Strong, Rebondable, Dynamic Cross-Linked Cellulose Nanocrystal Polymer Nanocomposite Adhesives, ACS Applied Materials & Interfaces 10, 30723-30731 (2018). http://dx.doi.org/10.1021/acsami.8b10520

[54] M. N. Dominguez, M. P. Howard, J. M. Maier, S. A. Valenzuela, Z. M. Sherman, J. F. Reuther, L. C. Reimnitz, J. Kang, S. H. Cho, S. L. Gibbs, A. K. Menta, D. L. Zhuang, A. van der Stok, S. J. Kline, E. V. Anslyn, T. M. Truskett, and D. J. Milliron, Assembly of Linked Nanocrystal Colloids by Reversible Covalent Bonds, Chemistry of Materials 32, 10235-10245 (2020). http://dx.doi.org/10.1021/acs.chemmater.0c04151

[55] S. Borsley and E. R. Kay, Dynamic covalent assembly and disassembly of nanoparticle aggregates, Chemical Communications 52, 9117-9120 (2016). http://dx.doi.org/10.1039/C6CC00135A

[56] Y. Wang, P. J. Santos, J. M. Kubiak, X. Guo, M. S. Lee, and R. J. Macfarlane, Multistimuli Responsive Nanocomposite Tectons for Pathway Dependent Self-Assembly and Acceleration of Covalent Bond Formation, Journal of the American Chemical Society 141, 13234-13243 (2019). http://dx.doi.org/10.1021/jacs.9b06695

[57] D. P. Nair, M. Podgórski, S. Chatani, T. Gong, W. Xi, C. R. Fenoli, and C. N. Bowman, The Thiol-Michael Addition Click Reaction: A Powerful and Widely Used Tool in Materials Chemistry, Chemistry of Materials 26, 724-744 (2014). http://dx.doi.org/10.1021/cm402180t

[58] I. M. Serafimova, M. A. Pufall, S. Krishnan, K. Duda, M. S. Cohen, R. L. Maglathlin, J. M. McFarland, R. M. Miller, M. Frödin, and J. Taunton, Reversible targeting of noncatalytic cysteines with chemically tuned electrophiles, Nature Chemical Biology 8, 471-476 (2012). http://dx.doi.org/10.1038/nchembio.925

[59] Y. Zhong, Y. Xu, and E. V. Anslyn, Studies of Reversible Conjugate Additions, European Journal of Organic Chemistry 2013, 5017-5021 (2013). http://dx.doi.org/https://doi.org/10.1002/ejoc.201300358

[60] E. H. Krenske, R. C. Petter, and K. N. Houk, Kinetics and Thermodynamics of Reversible Thiol Additions to Mono- and Diactivated Michael Acceptors: Implications for the Design of Drugs That Bind Covalently to Cysteines, The Journal of Organic Chemistry 81, 11726-11733 (2016). http://dx.doi.org/10.1021/acs.joc.6b02188

[61] K. M. Herbert, N. D. Dolinski, N. R. Boynton, J. G. Murphy, C. A. Lindberg, S. J. Sibener, and S. J. Rowan, Controlling the Morphology of Dynamic Thia-Michael Networks to Target Pressure-Sensitive and Hot Melt Adhesives, ACS Applied Materials & Interfaces 13, 27471-27480 (2021). http://dx.doi.org/10.1021/acsami.1c05813

[62] T. M. FitzSimons, F. Oentoro, T. V. Shanbhag, E. V. Anslyn, and A. M. Rosales, Preferential Control of Forward Reaction Kinetics in Hydrogels Crosslinked with Reversible Conjugate Additions, Macromolecules 53, 3738-3746 (2020). http://dx.doi.org/10.1021/acs.macromol.0c00335

[63] T. M. FitzSimons, E. V. Anslyn, and A. M. Rosales, Effect of pH on the Properties of Hydrogels Cross-Linked via Dynamic Thia-Michael Addition Bonds, ACS Polymers Au (2021). http://dx.doi.org/10.1021/acspolymersau.1c00049

[64] C. I. C. Crucho, C. Baleizão, and J. P. S. Farinha, Functional Group Coverage and Conversion Quantification in Nanostructured Silica by 1H NMR, Analytical Chemistry 89, 681-687 (2017). http://dx.doi.org/10.1021/acs.analchem.6b03117

[65] P. Coussot, Q. D. Nguyen, H. T. Huynh, and D. Bonn, Viscosity bifurcation in thixotropic, yielding fluids, Journal of Rheology 46, 573-589 (2002). http://dx.doi.org/10.1122/1.1459447

[66] G. Ovarlez, L. Tocquer, F. Bertrand, and P. Coussot, Rheopexy and tunable yield stress of carbon black suspensions, Soft Matter 9, 5540-5549 (2013). http://dx.doi.org/10.1039/C3SM27650C

[67] H. A. Barnes, Thixotropy—a review, Journal of Non-Newtonian Fluid Mechanics 70, 1-33 (1997). http://dx.doi.org/https://doi.org/10.1016/S0377-0257(97)00004-9

[68] J. H. Maas, G. J. Fleer, F. A. M. Leermakers, and M. A. Cohen Stuart, Wetting of a Polymer Brush by a Chemically Identical Polymer Melt: Phase Diagram and Film Stability, Langmuir 18, 8871-8880 (2002). http://dx.doi.org/10.1021/la020430y

[69] D. L. Green and J. Mewis, Connecting the Wetting and Rheological Behaviors of Poly(dimethylsiloxane)-Grafted Silica Spheres in Poly(dimethylsiloxane) Melts, Langmuir 22, 9546-9553 (2006). http://dx.doi.org/10.1021/la061136z

[70] N. Dutta and D. Green, Nanoparticle Stability in Semidilute and Concentrated Polymer Solutions, Langmuir 24, 5260-5269 (2008). http://dx.doi.org/10.1021/la7027516

[71] D. Dukes, Y. Li, S. Lewis, B. Benicewicz, L. Schadler, and S. K. Kumar, Conformational Transitions of Spherical Polymer Brushes: Synthesis, Characterization, and Theory, Macromolecules 43, 1564-1570 (2010). http://dx.doi.org/10.1021/ma901228t

[72] K. Ohno, T. Morinaga, S. Takeno, Y. Tsujii, and T. Fukuda, Suspensions of Silica Particles Grafted with Concentrated Polymer Brush: Effects of Graft Chain Length on Brush Layer Thickness and Colloidal Crystallization, Macromolecules 40, 9143-9150 (2007). http://dx.doi.org/10.1021/ma071770z

[73] D. C. Pozzo and L. M. Walker, Reversible shear gelation of polymer–clay dispersions, Colloids and Surfaces A: Physicochemical and Engineering Aspects 240, 187-198 (2004). http://dx.doi.org/https://doi.org/10.1016/j.colsurfa.2004.04.040

[74] Y. Otsubo and K. Umeya, Rheological Properties of Silica Suspensions in Polyacrylamide Solutions, Journal of Rheology 28, 95-108 (1984). http://dx.doi.org/10.1122/1.549742

[75] B. Cabane, K. Wong, P. Lindner, and F. Lafuma, Shear induced gelation of colloidal dispersions, Journal of Rheology 41, 531-547 (1997). http://dx.doi.org/10.1122/1.550874

[76] J. Zebrowski, V. Prasad, W. Zhang, L. M. Walker, and D. A. Weitz, Shake-gels: shear-induced gelation of laponite–PEO mixtures, Colloids and Surfaces A: Physicochemical and Engineering Aspects 213, 189-197 (2003). http://dx.doi.org/https://doi.org/10.1016/S0927-7757(02)00512-5

[77] H. Collini, M. Mohr, P. Luckham, J. Shan, and A. Russell, The effects of polymer concentration, shear rate and temperature on the gelation time of aqueous Silica-

Poly(ethylene-oxide) “Shake-gels”, Journal of Colloid and Interface Science 517, 1-8 (2018). http://dx.doi.org/https://doi.org/10.1016/j.jcis.2018.01.094

[78] H. Kanai and T. Amari, Negative thixotropy in ferric-oxide suspensions, Rheologica Acta 34, 303-310 (1995). http://dx.doi.org/10.1007/BF00396021

[79] J. B. Yannas and R. N. Gonzalez, A Clear Instance of Rheopectic Flow, Nature 191, 1384-1385 (1961). http://dx.doi.org/10.1038/1911384a0

[80] F. R. Kersey, W. C. Yount, and S. L. Craig, Single-Molecule Force Spectroscopy of Bimolecular Reactions: System Homology in the Mechanical Activation of Ligand Substitution Reactions, Journal of the American Chemical Society 128, 3886-3887 (2006). http://dx.doi.org/10.1021/ja058516b

[81] F. R. Kersey, D. M. Loveless, and S. L. Craig, A hybrid polymer gel with controlled rates of cross-link rupture and self-repair, Journal of The Royal Society Interface 4, 373-380 (2007). http://dx.doi.org/10.1098/rsif.2006.0187

[82] E. Guazelli and J. F. Morris, *A Physical Introduction to Suspension Dynamics*, Cambridge University Press, New York, 2012. Isbn-13: 978-0521149273

[83] J. F. Morris, Lubricated-to-frictional shear thickening scenario in dense suspensions, Physical Review Fluids 3, 110508 (2018). http://dx.doi.org/10.1103/PhysRevFluids.3.110508

[84] J. E. Thomas, K. Ramola, A. Singh, R. Mari, J. F. Morris, and B. Chakraborty, Microscopic Origin of Frictional Rheology in Dense Suspensions: Correlations in Force Space, Physical Review Letters 121, 128002 (2018). http://dx.doi.org/10.1103/PhysRevLett.121.128002

[85] R. Mari, R. Seto, J. F. Morris, and M. M. Denn, Shear thickening, frictionless and frictional rheologies in non-Brownian suspensions, Journal of Rheology 58, 1693-1724 (2014). http://dx.doi.org/Doi 10.1122/1.4890747

[86] A. Singh, R. Mari, M. M. Denn, and J. F. Morris, A constitutive model for simple shear of dense frictional suspensions, Journal of Rheology 62, 457-468 (2018). http://dx.doi.org/10.1122/1.4999237

[87] N. Estrada, E. Azema, F. Radjai, and A. Taboada, Identification of rolling resistance as a shape parameter in sheared granular media, Physical Review E 84, 011306 (2011). http://dx.doi.org/10.1103/Physreve.84.011306

[88] A. Singh, C. Ness, R. Seto, J. J. de Pablo, and H. M. Jaeger, Shear thickening and jamming of dense suspensions: the roll of friction, Physical Review Letters 124, 248005 (2020). http://dx.doi.org/10.1103/PhysRevLett.124.248005

[89] N. Y. Lin, C. Ness, M. E. Cates, J. Sun, and I. Cohen, Tunable shear thickening in suspensions, Proc Natl Acad Sci U S A 113, 10774-10778 (2016). http://dx.doi.org/10.1073/pnas.1608348113